Packaging-Induced Strain Measurement Based on the Degree of Polarization in GaAsP–GaInP High-Power Diode Laser Bars

Ye Wang, Li Qin, Yan Zhang, Zhenhua Tian, Ye Yang, Zaijin Li, Chao Wang, Di Yao, Honghe Yin, Yun Liu, and Lijun Wang

***Abstract*—The strain caused by device packaging was studied in high-power semiconductor laser bars by measuring the degree of polarization. Polarization measurement with intentionally GaAsP–GaInP strained laser bar packaged on a Cu heat sink for 799-nm emission revealed the variation of band edges between the conduction band and heavy-hole or light-hole bands in the active region. This served as a method for evaluating the strain. In the packaging process, a maximum of 1800-ppm strain was transmitted to the active region. It was found that the defect density of 14.3% was induced.**

***Index Terms*—Laser modes, semiconductor device packaging, semiconductor laser arrays, strain measurement.**

I. Introduction

HIGH-POWER diode lasers offer wide potential applications such as industrial materials processing [1], printing, and medical applications as versatile light sources. Today, continuous-wave (CW) output power of laser bars using indium solder have been in excess of 1000 W [2]. However, indium solder called “soft solder” would induce the strain and defects that limit the lifetime as well as emission power, and induce the “smile” effect which cumbers beam shaping and fiber coupling of diode lasers. Thus, for more reliable devices, packaging techniques including architectures with less strain and defects are the primary aim. Simultaneously, the measurement of strain and defects are required urgently.

Tomm and Gerhardt *et al.* have put forward some approaches about the packaging-induced strain and defects utilizing optical techniques: microphotoluminescence [3], [4], photocurrent spectroscopy [5]–[8], and electroluminescence microscopy [9]. Reference [9] has demonstrated that the degree of polarization could show the qualitative information for the strain, but it did not include the absolute values of strain. In this letter, we demonstrate that strain values can be derived from the degree of polarization for GaAsP strained laser bars.

Manuscript received December 08, 2008; revised March 10, 2009. First published May 05, 2009; current version published June 24, 2009.

The authors are with the Laboratory of Excited State Processes, Changchun Institute of Optics, Fine Mechanics and Physics, Chinese Academy of Sciences, Changchun 130033, China (e-mail: wy19812005@163.com; qinl@ciomp.ac.cn; qhdzhangyan@gmail.com; greathailang@163.com; yangyy0719@163.com; lizaijin@126.com; freebaige@163.com; ydchina431@xina.com; yinhh5678@sina.com; liuy@ciomp.ac.cn; wanglj@ciomp.ac.cn).

Digital Object Identifier 10.1109/LPT.2009.2021148

II. Experimental Approach and Laser Structure

The degree of polarization (ρ) is determined from the tensile-strained quantum-well (QW)

$$\begin{aligned}\rho &= (P_{\rm TM} - P_{\rm TE})/(P_{\rm TM} + P_{\rm TE})\\ &= (P_{\rm TM}/P_{\rm TE} - 1)/(P_{\rm TM}/P_{\rm TE} + 1)\end{aligned} \quad (1)$$

where $P_{\rm TE}$ and $P_{\rm TM}$ are the respective powers of nearly transverse-electric (TE) modes and nearly transverse-magnetic (TM) modes. The output power (P) of laser bars operated under the threshold current is given by [10]

$$P = \eta_r \eta_i \alpha_m/(\alpha_m + \alpha_i) h\nu/q\beta_{\rm sp} I \quad (2)$$

where η_i is the internal differential quantum efficiency, α_m is the mirror loss and α_i represents all internal losses, I is the operation current, ν is the frequency of the emitted photons, $\beta_{\rm sp}$ is the spontaneous emission transition factor, and η_r is the radiation efficiency, which can be given by [10]

$$\eta_r = R_{\rm sp}/(\eta_i I/(qV)). \quad (3)$$

Here, V represents the volume of the active region. Under the threshold current, spontaneous emission transition rate $R_{\rm sp}$ is written by [11]

$$R_{\rm sp} = A m_r^*/(d\pi\hbar^2) f(E_2)[1 - f(E_1)] \quad (4)$$

Here m_r^* is the effective mass of oscillator, d is the thickness of QW, A is the proportionality constant for spontaneous emission, and $f(E_2), f(E_1)$ are the Fermi–Dirac distribution functions for the electrons in the conduction band with the energy E_2 and the ones in the valence band with the energy E_1. So combing (2)–(4), a simplified expression is reached

$$\begin{aligned}P_{\rm TM}/P_{\rm TE} = c^2 E_{q\rm TM}^5/E_{q\rm TE}^5\\ \cdot \exp[2(E_{q\rm TE} - E_{q\rm TM})/kT]\end{aligned} \quad (5)$$

where

$$c = m_{\rm lh}^* \cdot (m_c^* + m_{\rm hh}^*) / [m_{\rm hh}^* \cdot (m_c^* + m_{\rm lh}^*)] \quad (6)$$

$$\begin{aligned}E_{qj} = E_{g0} + \Delta E_j + \hbar^2/(2m_c^*)(\pi/d)^2\\ + \hbar^2/(2m_j^*)(\pi/d)^2, j = {\rm TE}, {\rm TM}\end{aligned} \quad (7)$$

$$m_{\rm TE}^* = m_{\rm hh}^*, m_{\rm TM}^* = m_{\rm lh}^*. \quad (8)$$

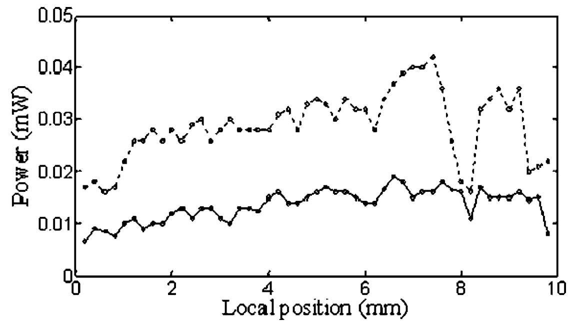

Fig. 1. Power curves of TE (full line) and TM (dotted line) modes of emitters along the GaAsP laser bar. The operation current is 4.2 A, about 30% of the laser threshold for this kind of device.

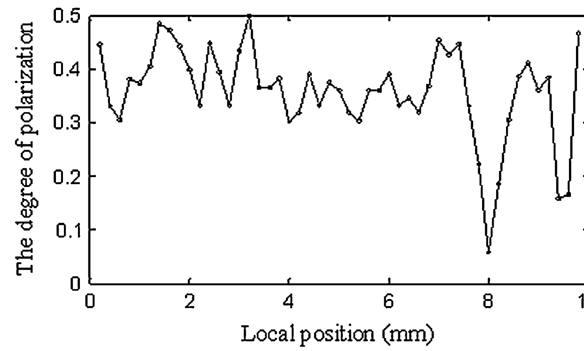

Fig. 2. Degree of polarization (ρ) versus local position. The result presented in this figure is determined from the data shown in Fig. 1.

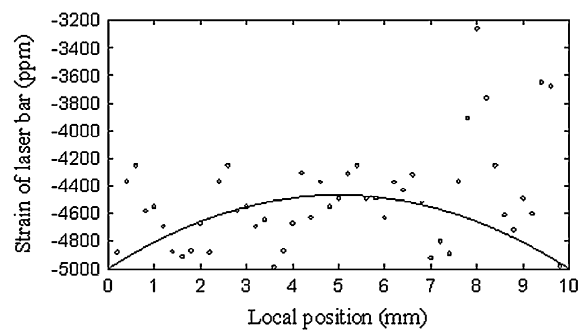

Fig. 3. Spatial variation (open circles) of the strain (ε) versus local position. These data are in good agreement with calculated strain profile.

E_{g0} represents the bandgap of natural materials of QW, $m_c^*, m_{\rm lh}^*, m_{\rm hh}^*$ represent the effective masses of electrons, light-hole and heavy-hole, respectively, and ΔE_j is related with the strain of laser bar; it can be written by [12]

$$\Delta E_j = a_j\varepsilon + b_j\varepsilon^2, j = \mathrm{TE}, \mathrm{TM} \tag{9}$$

where a_j, b_j are the constants for the fixed QW and ε is the strain value.

In the experiment, we studied a 799-nm diode laser bar packaged on a Cu heat sink. The laser chip was grown by metal–organic chemical vapor deposition on an n-type GaAs substrate and consisted of 10-nm tensile-strained GaAsP single QW, which was sandwiched between the GaInP waveguide layers. The chip dimensions were 130 μm (total thickness) $\times$ 1 mm (cavity length) $\times$ 1 cm (total lateral width). The bar contained 49 emitters with a width of 100 μm separated by 100-μm-wide optical and electrical isolation regions. It was mounted p-side down on a Cu heat sink with indium solder. Soldering was completed by Diomount MKIII system for the mounting of high-performance diode laser bars. The position of the bar picked up by a very precise and flat vacuum tool was controlled by multiaxis alignment stages and an optical control with adapted image-processing software. After the position was adjusted, the bar was brought to the integrated reflow oven, the bar and heat sink were soldered together using shielding gas.

The highest power of 60 W could be achieved at 72 A under CW operation at 300 K. The threshold current was 13.4 A, and the slope efficiency was 1.03 A/W. In order to avoid thermal and carrier redistribution effects, the device was operated at 4.2 A, which was about 30% of the threshold current. The power signals were measured by a Spectra-Physics 404 power meter. The device, fixed on an adjustable temperature stabilized heat sink ($T = 300$ K), was moved along the aperture of the power meter. A 200-μm-wide slit was situated in front of the bar. The step length was 200 μm. A polarization beam splitter was allowed for separating TM and TE polarizations. The accurate alignment of the test device was done using a HeNe laser light beam which got reflected from the front facet of the device. The degree of polarization could be measured reproducibility in ± 0.0005.

III. Results

Fig. 1 shows powers of TE and TM modes below laser threshold, $P_{\rm TE}$ (full line) and $P_{\rm TM}$ (dotted line) versus the local position for GaAsP laser bar. In Fig. 2, the degree of polarization, calculated according to (1), is given. Referring to (1), (6)–(9), and the data shown in Fig. 2, taking no account of nonuniform current distributions along the laser bar, we can obtain the data about the strain (circles) shown in Fig. 3. For naked $\mathrm{GaAs_{0.86}P}$ bar, the original strain $\varepsilon = -5000$ ppm [13], obviously the strain differences between the experimental data and the original strain, are caused by the packaging process. After soldering, the laser bar and Cu heat sink cool down from the soldering temperature to ambient temperature synchronously. Due to the different thermal expansion coefficients of laser bar and Cu heat sink, the laser bar is compressed by heat sink; the packaging-induced strain is induced to the active region and compensates the original strain. About 800-ppm packaging-induced strain is transmitted to the active region at the center of laser bar, but the packaging-induced strain is nearly zero at $x = 0, 10$ mm, which shows a complete strain relaxation towards the device edges. The increased packaging-induced strain at the center of laser bar arouses the decreased split between heavy-hole and light-hole-valence-band in the QW of the laser structure. This leads to an increased hole population of states in the heavy-hole band consequently increases TE emission, so the degree of polarization decreases towards the center of the bar. Thus, the measurement of the degree of polarization can be used as a convenient method for strain in QW devices.

The experimental data are compared to the results of a model calculation (line) in Fig. 3 by ANSYS software that holds out a two-dimensional solid element model (PLANE 82) for the laser bar with a width of 1 cm and a cavity length of merely 1 mm, which can apply in not only elastically strained systems but also a very thin (10 μm) viscoelastic solder layer substantially.

TABLE I
PARAMETERS OF LASER DIODE

Layer	Young's Modulus (GPa)	Poisson's ratio	Thermal expansion Coefficient ($10^{-5} K^{-1}$)
GaAs	85	0.31	0.65
In	11	0.486	3.21
Cu	110	0.34	1.65

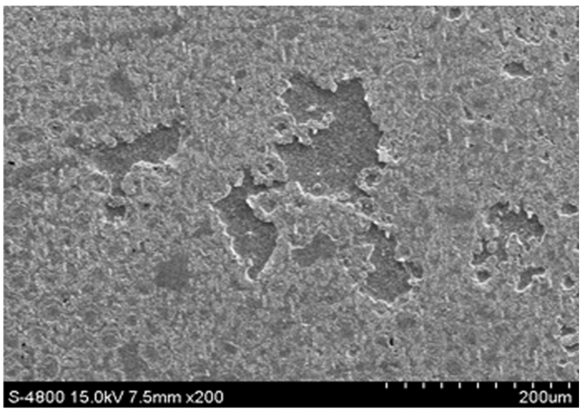

Fig. 4. SEM micrograph of the edge of laser bar.

In order to calculate the strain of the semiconductor crystal along the lateral direction of the laser bar $(\Delta x/x)$, isotropy in the epitaxial layer plane is assumed and the shearing strain $(\varepsilon_{xy}, \varepsilon_{yz}, \varepsilon_{xz})$ can be ignored; the predominant biaxial strain in the plane can be described by a strain ε with the tensor components $-\varepsilon = \varepsilon_{xx} = \varepsilon_{yy}$. Such an assumption should be considered in the experimental data, too. In model calculation procedure, we choose the structure analysis. After creating the laser model and defining parameters of each layer, we mesh different elements freely with different smart sizes in the model. We assume no strain in 156 °C; the model calculation is simulated when the solder temperature of 156 °C is loaded on the laser bar while the room temperature of 25 °C is loaded on the heat sink as boundary conditions without the consideration of strain/temperature dependency. Fig. 3 gives a comparison between data of theoretical analysis and an experiment which shows basic agreement. Table I lists the parameters of each layer of the diode laser.

The strain values of the right emitters show more variation apparently. It is possibly because the defects, such as voids or cracks, are created in the solder layer. In order to confirm this hypothesis, we performed scanning electron microscope (SEM) measurements of indium solder layers of a mass of other diode lasers, which were manufactured in the same packaging conditions. The defects are certain to exist at the edge of laser bars. Fig. 4 is one of the micrographs. In Fig. 3, about 1/7 of the emitters of the laser bar, namely 14.3% of defect density, are affected by these defects. A maximum of 1800-ppm strain is transmitted to the active region at the right edge of laser bar.

IV. CONCLUSION

For high-power diode lasers, chip soldering is a central issue lastingly due to packaging-induced strain and defects which affect the laser parameters as well as lifetime and reliability of the device. So the measurements of both defect and strain are necessary. We have demonstrated the measurement of the degree of polarization could be used as a convenient method for strain and defects in QW devices, the results basically agreed with the model calculation. The packaging-induced strain was transmitted towards the active region through solder layer due to the different thermal expansion coefficients of laser bar and heat sink. A maximum of 1800-ppm packaging-induced strain was transmitted to the active region at the right edge of laser bar. It was also found that the defect density of 14.3% was induced synchronously.

REFERENCES

[1] F. G. Bachmann, "Application adapted diode laser systems a result of the German national research project "MDS"," *Proc. SPIE*, vol. 4973, pp. 68–76, 2003.

[2] H. Li, I. Chyr, D. Brown, F. Reinhardt, O. Romero, C. H. Chen, R. Miller, K. Kuppuswamy, X. Jin, T. Nguyen, T. Towe, T. Crum, C. Mitchell, T. Truchan, R. Bullock, E. Wolak, J. Mott, and J. Harrison, "Next-generation high-power, high-efficiency diode lasers at spectra-physics," *Proc. SPIE*, vol. 6824, pp. 68240S-1–68240S-12, 2008.

[3] R. Xia, E. C. Larkins, I. Harrison, S. R. A. Dods, A. Andrianov, J. Morgan, and J. P. Landesman, "Mounting-induced strain threshold for the degradation of high-power AlGaAs laser bars," *IEEE Photon. Technol. Lett.*, vol. 14, no. 7, pp. 893–895, Jul. 2002.

[4] P. Martin, J. P. Landesman, E. Martin, A. Fily, J. P. Hirtz, and R. Bisaro, "Micro-photoluminescene mapping of packaging-induced stress distribution in high-power AlGaAs laser diodes," *Proc. SPIE*, vol. 3945, pp. 308–316, 2000.

[5] J. W. Tomm, R. Müller, A. Bärwolff, T. Elsaesser, D. Lorenzen, and F. X. Daiminger, "Direct spectroscopic measurement of mounting-induced strain in high-power optoelectronic devices," *Appl. Phys. Lett.*, vol. 73, pp. 3908–3910, Dec. 1998.

[6] J. W. Tomm, R. Müller, A. Bärwolff, T. Elsaesser, A. Gerhardt, J. Donec-ker, D. Lorenzen, F. X. Daiminger, S. Weiß, M. Hutter, E. Kaulfersch, and H. Reichl, "Spectroscopic measurement of packaging-induced strains in quantum well laser diodes," *J. Appl. Phys.*, vol. 86, pp. 1196–1201, Aug. 1999.

[7] J. W. Tomm, A. Bärwolff, T. Elsaesser, and J. Luft, "Selective excitation and photoinduced bleaching of defects in InAlGaAs/GaAs high-power diode lasers," *Appl. Phys. Lett.*, vol. 77, pp. 747–749, Jul. 2000.

[8] J. W. Tomm, A. Gerhardt, T. Elsaesser, D. Lorenzen, and P. Hennig, "Simultaneous quantification of strain and defects in high-power diode laser devices," *Appl. Phys. Lett.*, vol. 81, pp. 3269–3271, Oct. 2002.

[9] J. W. Tomm, A. Gerhardt, R. Müller, V. Malyarchuk, Y. Sainte-Marie, P. Galtier, J. Nagle, and J.-P. Landesman, "Spatially resolved spectroscopic strain measurements on high-power laser diode bars," *J. Appl. Phys.*, vol. 93, pp. 1354–1362, Feb. 2003.

[10] L. A. Coldren and S. W. Corzine, *Diode Lasers and Photonic Integrated Circuits*. Hoboken, NJ: Wiley, 1995, ch. 2.

[11] B. Du, *The Principle of Diode Lasers*. Beijing: Weapons & Industry, 2004, ch. 2.

[12] L. A. Coldren and S. W. Corzine, *Diode Lasers and Photonic Integrated Circuits*. Hoboken, NJ: Wiley, 1995, pp. 368–372.

[13] L. A. Coldren and S. W. Corzine, *Diode Lasers and Photonic Integrated Circuits*. Hoboken, NJ: Wiley, 1995, Appendix 11.